

1 **Current estimates of biogenic emissions from Eucalypts**

2 **uncertain for Southeast Australia**

3 K.M. Emmerson¹, I.E. Galbally¹, A.B. Guenther², C. Paton-Walsh³, E-A. Guerette³, M.E.
4 Cope¹, M.D. Keywood¹, S.J. Lawson¹, S.B. Molloy¹, E. Dunne¹, M. Thatcher¹, T. Karl⁴, S.D.
5 Maleknia⁵

6 1 CSIRO Oceans & Atmosphere, PMB1, Aspendale, VIC, Australia.

7 2 Department of Earth System Science, University of California, Irvine, USA.

8 3 Centre for Atmospheric Chemistry, School of Chemistry, University of Wollongong, Wollongong, NSW,
9 Australia.

10 4 Institute of Atmospheric and Cryospheric Sciences, University of Innsbruck, Innsbruck, Austria.

11 5 Centre for Ecosystem Science, School of Biological, Earth and Environmental Sciences, University of New
12 South Wales, Australia.

13 *Correspondence to:* K.M. Emmerson (kathryn.emmerson@csiro.au)

14

15 **Abstract.** The biogenic emissions of isoprene and monoterpenes are one of the main drivers of atmospheric
16 photochemistry, including oxidant and secondary organic aerosol production. In this paper, the emission rates of
17 isoprene and monoterpenes from Australian vegetation are investigated for the first time using the Model of
18 Emissions of Gases and Aerosols from Nature version 2.1 (MEGANv2.1), the CSIRO chemical transport model,
19 and atmospheric observations of isoprene, monoterpenes and isoprene oxidation products (methacrolein and
20 methyl-vinyl-ketone). Observations from four field campaigns during three different seasons are used, covering
21 urban, coastal suburban and inland forest areas. The observed concentrations of isoprene and monoterpenes were
22 of a broadly similar magnitude, which may indicate that southeast Australia holds an unusual position where
23 neither chemical species dominates. The model results overestimate the observed atmospheric concentrations of
24 isoprene (up to a factor of 6) and underestimate the monoterpene concentrations (up to a factor of 4). This may
25 occur because the emission rates currently used in MEGANv2.1 for Australia are drawn mainly from young
26 Eucalypt trees (<7yrs), which may emit more isoprene than adult trees. There is no single increase/decrease factor
27 for the emissions which suits all seasons and conditions studied. There is a need for further field measurements of
28 in-situ isoprene and monoterpene emission fluxes in Australia.

29

30 **1 Introduction**

31 Biogenic volatile organic compounds (BVOCs) originate from terrestrial and marine ecosystems, and have an
32 annual flux of approximately 1150 Tg C yr⁻¹ (Guenther et al., 1995). Almost 90% of BVOCs are emitted from
33 plants and trees, with the most dominant species being isoprene and monoterpenes (Lathiere et al., 2006; Guenther
34 et al., 2012). The isoprene and monoterpene emission rates from vegetation are determined by a combination of
35 environmental factors (light, temperature, water stress etc.) and genetic make-up of the species being considered
36 (Guenther et al., 2012). In regions of dense vegetation these BVOCs dominate the oxidative capacity of the

1 atmosphere (Houweling et al., 1998; Taraborrelli et al., 2012), and are important in the production of ozone
2 (Simpson, 1995; Pierce et al., 1998) and secondary organic aerosol (Hoffmann et al., 1997; Griffin et al., 1999;
3 van Donkelaar et al., 2007).

4 Concentrations of BVOCs in the atmosphere are a function of the emission rate from the underlying vegetation,
5 the mixing depth of the boundary layer, entrainment rate at the top of the boundary layer, horizontal advection,
6 and the rate of removal within the boundary layer by the hydroxyl and nitrate radicals, and ozone. All of these
7 processes vary diurnally. Modern chemical transport models can simulate all these processes provided they include
8 an emission module for BVOCs such as the Model of Emissions of Gases and Aerosols from Nature (MEGAN).

9 MEGAN was developed to provide a parameterisation for BVOC emissions applicable over the Earth's surface
10 (Guenther et al., 2012; Guenther et al., 2006; Guenther et al., 1995). MEGAN uses meteorological parameters such
11 as temperature and solar radiation, land use maps incorporating vegetation and land cover, and emission factors
12 based on global observations of plant responses to light and temperature. MEGAN has been incorporated and run
13 within a number of global chemistry models (Guenther et al., 2006; Heald et al., 2008; Emmons et al., 2010; Millet
14 et al., 2010; Pfister et al., 2008), and for regional air quality studies (Situ et al., 2013; Stavrakou et al., 2014; Kim
15 et al., 2014). Sensitivity studies on the input data for MEGAN have highlighted the importance of time and spatial
16 resolution in meteorological data (Ashworth et al., 2010; Arneth et al., 2011). A comparison of isoprene emissions
17 driven by low resolution (degree scale) and high resolution (10km) meteorological fields showed changes up to
18 150% due to smoothing via averaging effects (Pugh et al., 2013). The importance of using accurate land cover data
19 in respect to the effects of isoprene on ozone concentrations has also been discussed (Kim et al., 2014), as has
20 changing all vegetation from default species to Eucalypts (Situ et al., 2013), which increased isoprene
21 concentrations by 315%.

22 There are over 700 species of Eucalypts native to Australia, many of which are expected to contribute to isoprene
23 emissions in the Southeast region. Evans et al. (1982) reported the first comprehensive survey of isoprene emission
24 and found that *Eucalyptus globulus* was the highest isoprene emitter of the 54 plant species examined. Eucalypts
25 were selected to be the subject of a number of subsequent isoprene emission studies and are considered as among
26 the highest isoprene emitting plants (e.g., Loreto and Delfine 2000). A small number of BVOC emission
27 measurements have been made in Australia, particularly of Eucalypt species (Winters et al., 2009; He et al., 2000),
28 flowering plants and pasture, including grass cutting (Kirstine et al., 1998) and tropical grasslands/woodlands
29 (Ayers and Gillett, 1988). Emissions from Eucalypt species outside Australia have been measured in the field
30 (Street et al., 1997), and the laboratory (Guenther et al., 1991).

31 Previous MEGAN predictions of BVOC emissions across Australia have had limited success. Muller et al. (2008)
32 found an overestimate of isoprene across northern Australia by comparing MEGANv2 to GOME satellite
33 measurements of formaldehyde, and in subsequent work estimated the magnitude of this over-prediction to be a
34 factor of 2-3 in January (Stavrakou et al., 2015). Sindelarova et al. (2014) found that reductions of 50% in
35 Australian isoprene emissions could be achieved by accounting for reduced isoprene emissions during low soil
36 moisture conditions.

37 The imperative for understanding biogenic emissions from Australia is clear as the country covers 22% of the land
38 area in the Southern Hemisphere (excluding Antarctica). This is the first high resolution regional study focussing

1 on whether the emission factors used in MEGAN are appropriate to represent BVOC emissions from diverse
2 locations in southeast Australia. We compare atmospheric concentrations of isoprene and monoterpenes observed
3 in these locations with concentrations modelled using MEGAN, the default emission factors and the CSIRO
4 chemical transport model. Sensitivity studies are undertaken on these emission factors. Tests on other variables to
5 assess model uncertainty are shown in the supplementary material. Differences between the modelled and
6 measured BVOCs are critically examined and the need for revised regional emission factors are evaluated.

7

8 **2 Materials and Methods**

9 **2.1 Field experiments**

10 Gas phase biogenic VOC data were measured using a Proton Transfer Reaction Mass Spectrometer (PTR-MS)
11 collected during four field experiments in areas of diverse land cover in southeast Australia. Figure 1 shows a map
12 giving the locations of the field campaign sites in southeast Australia, showing their proximity to the coast and
13 urban regions, and forested areas. Data within Figure 1 are discussed later. The PTR-MS measures groups of
14 species which correspond to certain mass to charge (m/z) ratios, for example isoprene, C_5H_8 , is identified at $m/z =$
15 69 (made up of the mass of C_5H_8 (68 g mol^{-1}) and a proton (1 g mol^{-1})). Whilst monoterpenes are identified at both
16 $m/z = 137$ and 81 (a dominant fragment produced by dissociative proton transfer), only the $m/z=137$ will be used.
17 The PTR-MS technique is ideal for developing and evaluating parameterisations for lumped species modelling as
18 most chemical mechanisms do not separate individual monoterpenes such as α - and β - pinenes, and conventional
19 gas chromatographic techniques may underestimate the actual monoterpene loading (Lee et al., 2005). Hourly
20 averages have been calculated from the PTR-MS data to be comparable to the time period of the modelled output.
21 For details of the PTR-MS measurements please refer to the citations given for each field campaign.

22 **2.1.1 The Sydney Particle Study**

23 The Sydney Particle Study (SPS) took place at Westmead, 33km to the west of Sydney centre (150.9961°E ,
24 33.8014°S) (Cope et al., 2014). The site is situated in a grassy field within the grounds of a psychiatric hospital.
25 Two intensive field campaigns took place, occurring between February 1st and March 7th 2011 (SPS1, summer)
26 and April 14th to May 14th 2012 (SPS2, autumn). The PTR-MS was operational from February 18th during SPS1,
27 and throughout the whole of SPS2. The height of the inlet was approximately 4m.

28 **2.1.2 MUMBA**

29 The Measurement of Urban, Marine and Biogenic Air (MUMBA) field campaign took place between December
30 21st 2012 and February 16th 2013 (summer) at the University of Wollongong eastern campus (150.8995°N ,
31 34.3972°S), about 80km to the south of Sydney (Paton-Walsh et al., submitted). Wollongong is a coastal location
32 with sharp gradients between marine, urban and forested regions. The PTR-MS instrument was situated in a hut
33 surrounded by a grass field, and sampled from a mast at a height of $\sim 10\text{m}$ above the surrounding ground level.

1 2.1.3 Tumbarumba

2 PTR-MS measurements were made for one week at Tumbarumba in New South Wales (148.1517°E, 35.6566°S)
3 between November 8th – 14th 2006 (late spring) (Maleknia, 2012; Maleknia et al., 2009). Tumbarumba is located
4 within the Bago State Forest and is surrounded by dominant Eucalypt species of *E. delagatensis* (Alpine Ash) and
5 *E. dalrympleana* (Mountain Gum) with an average height of 40m. Isoprene and monoterpenes were observed from
6 an inlet height of 45m. Despite being late spring the campaign experienced snowstorm conditions that caused
7 damage to the trees. This resulted in a four-fold increase to the emissions of monoterpenes whilst isoprene levels
8 remained low due to cold temperatures (~8°C) (Maleknia et al., 2009). Three days of eddy covariance flux
9 measurements are available for isoprene and monoterpenes from the post-storm period at Tumbarumba. These
10 data will provide a direct constraint on modelled emissions despite being caveated by the unusual vegetation stress
11 response.

12 2.2 The Modelling Framework

13 The CSIRO Chemical Transport Model (CTM) has been developed over 15 years for Australian regional air quality
14 issues (Cope et al., 2004). The CTM is a three-dimensional Eulerian chemical transport model with 35 levels in
15 the vertical to 40km. The CTM has the capability of modelling the emissions, transport, chemical transformation,
16 wet and dry deposition of a coupled gas and aerosol phase atmospheric system. The modelling uses a nested
17 approach, downscaling from global background concentrations which are advected into the Australian region by
18 the prevailing winds. The Australia-wide domain at 80km resolution is used to simulate the transport of species
19 from large scale continental processes that feed into the boundary conditions of three successively smaller nested
20 grids. The highest resolution grid (3km) has a domain size of 180 x 180 km and is centred on each field campaign
21 site.

22 The CTM is driven by meteorology from the Conformal Cubic Atmospheric Model (CCAM, (McGregor and Dix,
23 2008)). CCAM is a global stretched grid dynamical model, used for the prediction of wind velocity, temperature,
24 water vapour mixing ratio (including clouds), radiation and turbulence. CCAM has been evaluated for use in
25 Australia and elsewhere (Corney et al., 2013; Nguyen et al., 2014). CCAM uses the Australian land surface
26 scheme, CABLE (Kowalczyk et al., 2013) to provide information on the surface roughness, soil moisture and leaf
27 area index (LAI, based on MODIS data). The soil moisture parameter has been evaluated indirectly within the
28 Global Soil Wetness Project, by comparing model evapotranspiration and runoff to measurements (Zhang et al.,
29 2013). Whilst CABLE performed well, soil moisture remains a source of uncertainty.

30 We have included MEGAN as an option in the CTM to calculate the biogenic emissions, the set-up of which is
31 described below. Anthropogenic emissions are based on the Sydney Greater Metropolitan Region inventory (NSW
32 Department of Environment, Climate Change and Water, now NSW EPA (DECCW, 2007)) and includes 37
33 species. The chemical transformation of gas-phase species is modelled using an extended version of the Carbon
34 Bond 5 mechanism (Sarwar et al., 2008) with updated toluene chemistry (Sarwar et al., 2011). The CB05
35 mechanism treats the production of a lumped isoprene oxidation product only, simplifying the chemistry. More
36 recent schemes consider explicit oxidation products which can affect the production of ozone and nitrate species.
37 The CB05 mechanism and its predecessor CBIV, have been compared with other schemes in Emmerson and Evans

1 (2009) and Knote et al. (2015), but not against measurements. Choice of chemistry scheme can introduce
2 uncertainty, which could be explored in future work. A two-bin sectional scheme calculates the aerosol
3 concentrations, using the Volatility Basis Set (Shrivastava et al., 2008) for the secondary organic species
4 partitioning, and ISORROPIA (Fountoukis and Nenes, 2007) for the inorganic partitioning. The CTM runs on a
5 chemical time step of 5 minutes with hourly output of all variables. Table 1 details how the model has been set up
6 and run, along with particulars of the sensitivity runs completed.

7 **2.3 Coupling MEGAN to the CSIRO CTM**

8 MEGAN was developed to provide a parameterisation for BVOC emissions and detailed descriptions can be found
9 in Guenther et al. (2012), with a useful review of modules given in Sindelarova et al. (2014). The most recent
10 version, MEGANv2.1 emits 147 species into 19 BVOC classes, which can be output into lumped species
11 appropriate for a number of popular chemical mechanisms, including the Carbon Bond 5 mechanism.

12 MEGANv2.1 is available as an offline code at <http://lar.wsu.edu/megan/guides.html>. The code is set-up for use
13 with the Weather Research and Forecasting (WRF) modelling system, but does not include the effect of CO₂ on
14 isoprene (Heald et al., 2009), nor the effects of soil moisture. Note that soil moisture is used elsewhere in the CTM
15 to calculate the dust emission flux, and could be coupled with MEGAN in the future. In this work, the MEGANv2.1
16 code has been extracted from the WRF system and coupled to the CSIRO CTM.

17 MEGANv2.1 provides two approaches for estimating emission factors. The first is to use the 16 plant functional
18 type (PFT) distributions and the global average PFT specific emission factors listed in Table 2 of Guenther et al.
19 (2012). In this case the emission rate, R ($\mu\text{g m}^{-2} \text{h}^{-1}$) of species i in any grid box, will be sensitive to the PFT
20 distributions used for the MEGAN simulation (Eq 1):

$$21 \quad R_i = \sum_{j=1}^{n_{PFT}} (EF_{ij} \times \gamma_{ij} \times \chi_j) \quad (1)$$

22 where EF_{ij} is the emission factor ($\mu\text{g m}^{-2} \text{h}^{-1}$) of species i under standard conditions for PFT j with fractional grid
23 box areal coverage χ_j . The emission activity factor γ_{ij} (dimensionless) accounts for emission control processes and
24 uses the following variables to drive the canopy model: compound class, response to light and temperature, leaf
25 age, soil moisture, CO₂ and LAI.

26 The second approach is to use MEGAN global emission factor maps, which are based on plant type composition
27 and plant type specific emission factors. In this case, the MEGAN simulation uses PFTs to define the canopy
28 environment characteristics and to define the fractional grid box areal coverage, but the results are not as sensitive
29 to the PFT data used. The emission rate, R for species i in a given grid cell, xy is (Eq 2):

$$30 \quad R_i = EF_{i,xy} \sum_{j=1}^{n_{PFT}} (\gamma_{ij} \times \chi_j) \quad (2)$$

31 This study uses both approaches, the latter approach for 10 species where emission factor maps are available, and
32 the former approach for all other species. Global emission factor maps (version 2011) for isoprene, myrcene,
33 sabinene, limonene, 3-carene, ocimene, α -pinene, β -pinene, 232-MBO (2-methyl-3-buten-2-ol) and NO are
34 provided at a 1km resolution with the MEGANv2.1 code download, and described below.

1 2.3.1 Production of Emission Factor maps for Australia

2 The MEGANv2.1 emission factor maps provide values for a specific location based on estimates of plant type
3 composition, which can be individual plant species or more general types, and emission factors for each plant type.
4 The global MEGAN PFT database was used to quantify the fraction of trees, shrubs, crops and herbs at each
5 location in Australia. The tree/shrub type composition for Australia was then determined from data compiled by
6 the Australian Department of Agriculture and Water Resources (DAWR) and released on the data.gov.au data
7 portal in 2003 (URL: <http://data.gov.au/dataset/forests-of-australia-2003>). The DAWR landcover data are
8 representative of the time period of 1996 to 2002 and include 20 categories. Australia has unusually low tree/shrub
9 genera diversity and many of these landscapes were represented in the DAWR database by a single tree/shrub
10 genera (e.g., *Acacia*, *Callitris*, *Casuarina*, *Eucalyptus*, *Melaleuca*) although some were more diverse (Mangrove,
11 Rainforest). The landscapes dominated by one genera were assigned the genera average emission factor in the
12 MEGAN plant type database. Mixed landscapes were assigned a representative plant type (e.g., the emission factor
13 for the genera *Avicennia* was assigned to trees in the Mangrove landscape).

14 The MEGANv2.1 emission factor database classifies *Eucalyptus* as a high emitter ($>10 \mu\text{g g}^{-1} \text{h}^{-1}$), *Casuarina* and
15 *Melaleuca* as moderate emitters ($1\text{-}10 \mu\text{g g}^{-1} \text{h}^{-1}$), and *Avicennia* and *Callitris* as very low emitters ($<1\mu\text{g g}^{-1} \text{h}^{-1}$).
16 Isoprene or monoterpene emissions have not been published for any Australian *Acacias* but eight *Acacia* species
17 from South Africa (Guenther et al., 1996; Harley et al., 2003) and the US (Guenther et al., 1999; Papiez et al.,
18 2009) have been investigated and only one isoprene emitter and one monoterpene emitter have been identified.
19 Based on these observations, the MEGAN model assumes low isoprene and monoterpene emission rates for
20 Australian *Acacia* species. The MEGANv2.1 isoprene emission factor for *Eucalyptus* was based on six enclosure
21 measurement studies (Evans et al., 1982; Winer et al., 1983; Guenther et al., 1991; Street et al., 1997; Loreto and
22 Delfine, 2000; He et al., 2000). Of these studies, only He et al. 2000 was conducted in Australia. These studies
23 report a large range of emission rates that are equivalent to MEGAN landscape emission factors of 1.6 to $51 \text{ mg g}^{-1} \text{h}^{-1}$.
24 Large variability (more than a factor of 3) was observed for different plants of the same *Eucalypt* species
25 measured in a single study (Guenther et al. 1991). The average isoprene emission factor of 15 *Eucalypt* species
26 measured by He et al. 2000, about $24 \text{ mg m}^{-2} \text{h}^{-1}$, was similar to the mean value for the other five studies and used
27 as the basis for assigning *Eucalypts* an isoprene emission factor of $24 \text{ mg m}^{-2} \text{h}^{-1}$. This is more than double the
28 isoprene emission factor used for broadleaf evergreen temperate trees if approach 2 is used (PFT sensitive).

29 The distribution of isoprene emission factors in southeast Australia are shown in Figure 1(a). The region between
30 Melbourne and Sydney is covered in vegetation emitting at the upper end of the map scale, close to $24 \text{ mg m}^{-2} \text{h}^{-1}$.
31

32 2.3.2 Meteorological and related inputs to MEGAN

33 The MEGAN canopy model requires photosynthetically active radiation (PAR), temperature, pressure, relative
34 humidity and LAI. CCAM supplies hourly temperature and PAR, which exhibit diurnal cycles with early afternoon
35 maxima. The hourly PAR is reduced by a cloud attenuation factor when conditions are cloudy. MEGAN also
36 requires an estimate of previous growing conditions, and needs 24 hour and 240 hour averaged temperature and
37 PAR. The 24 hour average of temperature is provided by CCAM. The 240 hour averaged temperature is fixed at

1 the observed average temperature for the duration of each campaign. The 24 hour averaged PAR is set using
2 measured solar radiation (in $W m^{-2}$) rather than CCAM output when measurements were available during the SPS2
3 and MUMBA campaigns. The observed and modelled PAR from the respective receptor sites are presented in
4 Figure 2. This calculation assumes PAR is half the total solar radiation fraction in the 400 – 700nm wavelength
5 band, and the conversion factor from $W m^{-2}$ to $\mu mol m^{-2} s^{-1}$ is 4.5. The model predicts the correct shape of the
6 diurnal profile but over-predicts by $126 \mu mol m^{-2} s^{-1}$ (7%) at noon during summer (MUMBA) and under-predicts
7 by $236 \mu mol m^{-2} s^{-1}$ (25%) during autumn (SPS2). Average campaign modelled PAR is used for SPS1 and
8 Tumarumba. Values for temperature and PAR are given in Table 1.

9 LAI data is provided from CCAM as described, at the same resolution as each model grid. The distribution of LAI
10 in summer (January) are shown in Figure 1(b), with high LAI data in the region of $5-6 m^2 m^{-2}$ in the coastal plains
11 and mountain ranges of southeast Australia.

12 2.3.3 Construction of high resolution PFT map for Australia

13 The Community Land Model PFT data from the NCAR data repository is provided on a $0.5^\circ \times 0.5^\circ$ resolution,
14 which when downscaled to the inner 3km grids for the CSIRO-CTM is not suitable (shown in Section 3.2). A new
15 PFT dataset has been constructed for this work, as 3km resolution data in the same format as the 16 PFTs required
16 by MEGAN is not available. A dataset from the International Geosphere Biosphere Project (IGBP) available at a
17 resolution of 1km with 17 landcover types (Belward et al., 1999) was used. The IGBP dataset was converted into
18 NCAR PFTs based on the schemes of Bonan et al. (2002), Poulter et al. (2011) and local knowledge. Bonan et al.
19 (2002) suggest how much bare ground should be introduced to each PFT grid cell, and also how best to split the
20 boreal from the temperate and tropical plant types using the average temperature of the coldest month. A 30 year
21 climatology of observed average winter temperatures (June - August) in Australia from the Bureau of Meteorology
22 was used for this purpose (www.bom.gov.au/jsp/awap).

23 Poulter et al (2011) noticed that IGBP classified much of Australia's interior with open shrublands. As a result,
24 'shrublands', 'grasslands' and 'savannahs' were split into a combination of shrubs and grass as per their
25 implementation in CABLE. Neither Bonan et al (2002) nor CABLE have vegetation occurring within 'urban'
26 landcover types, which would lead to zero biogenic VOC emissions in Sydney within this high resolution
27 implementation. An estimate of vegetation cover in Australian urban areas was made based on Kirstine and
28 Galbally (2004). Table S1 in the supplementary material gives details of how the IGBP landcover dataset was split
29 into the NCAR 16 PFTs suitable for MEGAN. Figure 3 shows the resulting spatial extent of the PFTs that
30 contribute at the field campaign sites. The maps show a high density (in most cases 95% coverage) of broadleaf
31 evergreen temperate trees around the coastal area. Shrubs and grasslands dominate the north west region, with
32 crops dominating the area in between.

33 3 Results

34 3.1 Contribution of plant functional types to emissions

35 We calculate the isoprene and monoterpene emission rates per plant functional type for each field campaign's
36 inner nested grids in the model (180 km x 180 km). The SPS and MUMBA grids are coastal and therefore contain

1 a high percentage of zero emitting ocean squares. The bar chart in Figure 4 shows the emission rate for isoprene
2 is an order of magnitude more than monoterpenes, and that broadleaf evergreen temperate trees dominate all
3 campaign airsheds. Tumbarumba is located near an agricultural region and is influenced by emissions from crops,
4 though whether these are croplands or pasture for animals is uncertain. The combination of high emission factors
5 and percentage of broadleaf evergreen temperate trees in the Tumbarumba grid (Eucalypts, section 2.1.3) enables
6 up to $3.2 \mu\text{g m}^{-2} \text{h}^{-1}$ of isoprene to be emitted (includes crop PFTs). A sensitivity study conducted for Tumbarumba
7 transferred 50% of the crop area to grassland. This resulted in reducing the peak isoprene by 0.5 – 0.7 ppb, but did
8 not affect the monoterpene concentrations.

9 **3.2 Comparisons of modelled and observed BVOCs**

10 Observed and modelled isoprene and monoterpenes are presented as time series for the four field campaigns in
11 Figure 5. Modelled isoprene is mostly over-predicted and monoterpenes mostly under-predicted. The model
12 captures the general peaks and troughs in the data, but at the wrong magnitude.

13 There are missing data from the observed SPS1 dataset and it is not obvious whether observed concentrations
14 would have risen further on 18-19th February 2011 as the model suggests. Also shown on the SPS1 time series
15 (Figure 5 top plots) are the results using the coarse 0.5×0.5 degree resolution PFT map. The very low
16 concentrations of isoprene (peak of 0.2 ppb) show that resolution of the input data is important, and recreating the
17 PFT maps was necessary.

18 Two of the first three modelled isoprene peaks in the MUMBA dataset (Figure 5 third plots down) coincide with
19 very hot ($>40^\circ\text{C}$) measured days. The first modelled isoprene peak on January 8th is 38 ppb at 43°C , yet the
20 observed peak is 5 ppb at 41°C . There may be isoprene inhibition at temperatures in excess of 40°C which is not
21 represented by the model (Guenther et al., 1991). January 8th is the only day CCAM predicts above 40°C during
22 MUMBA, whilst observations on the 8th and 18th are also above 40°C . CCAM predicts 33°C on the 18th leading to
23 modelled isoprene of 7 ppb; the observations show 4.5 ppb at 44°C . The modelled peak of 8 ppb at 32°C on
24 January 12th is not mirrored by an observed peak. Whilst temperatures were hot throughout NSW on January 12th,
25 a sea-breeze kept Wollongong cooler at 25°C . The modelled monoterpene Tumbarumba dataset has a number of
26 peaks not seen in the observations (Figure 5 bottom plots).

27 Figure 6 shows the eddy covariance flux measurements of isoprene and monoterpenes from the post-storm period
28 at Tumbarumba. Uncertainty in the night-time observations are 40% because advection terms were not well
29 constrained, however the daytime fluxes that dominate are within typical levels of uncertainty. The observed
30 diurnal cycles are compared to modelled emission flux data for the same time period in Figure 6. These
31 observations show peak monoterpene fluxes under $0.8 \text{ mg m}^{-2} \text{h}^{-1}$ at a time when the monoterpene response
32 increased by a factor of four as a result of the storm (Maleknia et al 2009). Observed isoprene fluxes peak under
33 $0.2 \text{ mg m}^{-2} \text{h}^{-1}$. The midday modelled emission rates over-predict the observed isoprene fluxes by a factor of 3,
34 and under-predict the monoterpene fluxes by a factor of 4. Comparing the emission fluxes directly gives confidence
35 that the modelled discrepancy is principally due to the emissions rather than model transport or chemical processes
36 (shown in the supplementary material).

1 Calculated ratios of emitted isoprene to monoterpene carbon were found to be 26.4 for forests in Michigan
2 (Kanawade et al., 2011) and 15.2 in the Amazon (Greenberg et al., 2004), both of which are isoprene dominated,
3 whilst forests in Finland (ratio = 0.18) are dominated by monoterpenes (Spirig et al., 2004). These Tumbarumba
4 data show a ratio of 0.14 highlighting the monoterpene dominance after the storm. If the storm had not taken place,
5 we suggest that isoprene and monoterpene emission fluxes would be broadly similar for both chemical species,
6 but more measurements are needed to confirm this. The magnitudes of the average observed isoprene and
7 monoterpene atmospheric concentrations are broadly similar for all four field studies, shown in Table 2. As
8 atmospheric concentrations are directly related to their emissions rates, the magnitudes of isoprene and
9 monoterpene emission fluxes must be similar under normal (non-storm) conditions, and the ratio of emitted
10 isoprene carbon to monoterpene carbon could be ~0.5-2. This phenomenon may be unique to southeast Australia.

11 Figure 7 shows campaign average diurnal time series for isoprene, monoterpenes and the ratio of carbon in isoprene
12 versus monoterpene atmospheric concentrations, comparing the CTM to the observations. In most cases the
13 MEGAN scheme predicts the shape of the diurnal profiles well, but isoprene is over-predicted during all four field
14 campaigns. A similar over-prediction in isoprene concentrations occurred using the CHIMERE model, run with
15 MEGANv2.04 at 9km resolution during the MUMBA campaign (Paton-Walsh et al., submitted).

16 The peak in modelled isoprene is over-predicted by factors between 2 and 6, which will have an effect through the
17 chemistry dependent on oxidant availability. The modelled isoprene profile captures the observed peak at 10am
18 seen at MUMBA in summer. The observed late afternoon peak in isoprene during SPS2 is diagnosed as due to a
19 collapsing autumnal boundary layer where oxidants at this time are depleted, but isoprene continues to be emitted.

20 The observed ratio of isoprene carbon versus monoterpene carbon peaks under ~2.5 at all four field studies. The
21 model over-predicts the observed ratio by factors between 3 and 10, the latter at MUMBA where lower
22 monoterpene concentrations were predicted compared with Sydney and Tumbarumba.

23 The modelled profile of monoterpenes generally matches the observed peaks for SPS1, SPS2 and MUMBA
24 campaigns, but the magnitude is under-predicted particularly at night by factors between 3 and 4. At Tumbarumba
25 the model predicts a similar monoterpene profile (peaks at night) to the other field campaigns, but the observations
26 show a light dependent profile, similar to isoprene. This could indicate plant stress due to storm damage occurring
27 that week (Harley et al., 2014). This process is not in the model.

28 Clearly, modelled isoprene is too high and monoterpenes are too low in southeast Australia. Sensitivity runs are
29 conducted to establish the magnitudes of emission corrections needed to achieve better model/observation
30 agreement. Emission factors for isoprene were reduced by a factor of 3. The emission factors for the monoterpenes
31 species myrcene, sabinene, limonene, 3-carene, ocimene, α -pinene and β -pinene were increased by a factor of 3.5.
32 Other monoterpene species remain unchanged as their concentrations do not dominate the total (Sindelarova et al.,
33 2014). The factors chosen are somewhat arbitrary. A decrease factor of 3 for isoprene suited the SPS1 profile best
34 whilst an increase of 3.5 suited the MUMBA monoterpenes profile best.

35 The modelled diurnal cycles from the emission factor sensitivity tests are shown as dashed red lines within Figure
36 7. The reduction in isoprene and increase in monoterpenes show better modelled agreement for most campaigns,
37 but particularly for isoprene in SPS1 and monoterpenes at MUMBA. The ratio of isoprene carbon to monoterpene

1 carbon concentrations from the emission factor sensitivity test give more reasonable results at MUMBA and
2 Tumbarumba, but under-predict the observed ratio for SPS1 and SPS2. Reducing the isoprene emission factors
3 has incurred a linear response in reducing the isoprene concentrations, but the factor of 3 used is not suitable for
4 all the field campaign data. At Tumbarumba, the reduction is likely a factor of 6. Similarly the monoterpene
5 increase by a factor of 3.5 does not suit all Australian conditions. Nevertheless, these results indicate the magnitude
6 of the corrections required.

7 Figure 8 shows quantile – quantile plots showing modelled and observed data ranked in ascending order. They
8 highlight any systematic biases that exist in the modelled data; if the modelled data were exactly like the
9 observations then the points would sit on the 1:1 line. Figure 8 shows the 1:1 line with two dashed lines
10 representing a factor of 2 either side. The aim is to further examine the extent of the over/under-prediction in
11 isoprene and monoterpenes. The data are paired; if the PTR-MS was offline then the modelled data is removed for
12 these times. The normalised mean bias is calculated; values closer to zero exhibit less bias.

13 There is a large model over-prediction in isoprene and therefore the isoprene products. Note that measurements of
14 isoprene products were not made available from Tumbarumba. The modelled monoterpenes are under-predicted
15 by just over a factor of 2 in most cases. The one exception is Tumbarumba which has zero model bias in
16 monoterpenes, however the shape of the modelled diurnal cycle was at odds with the observed profile. The results
17 from the emission factor sensitivity test show better modelled isoprene profiles, but the factor of 3.5 increase in
18 monoterpene emissions is too high. The bias in modelled VOCs is reduced in the emission factor sensitivity test.
19 For isoprene the bias switches from positive to negative indicating the chosen decrease factor is too high. The
20 increase factor for monoterpenes is too high for SPS1 and SPS2, both of which show equal sized biases but with
21 the opposite sign to the bias in the base case run.

22 The concentrations of the isoprene products can also be used to evaluate the lifetime of isoprene in the model and
23 observations. Figure 9 shows the ratio of isoprene and its products to the isoprene products. This examines whether
24 the model chemistry is proceeding at observed rates. The results show high correlations >0.85 for the observed
25 ratios; correlations in excess of 0.90 for SPS1 and SPS2 for species modelled by the base case run; and less well
26 correlated (>0.78) in the modelled base case at MUMBA. More isoprene products are predicted by the model than
27 the observations for SPS1. This suggests that oxidation occurs faster in the model compared to the observations
28 for February 2011. However the modelled rates of oxidation are more reasonable for SPS2 and MUMBA. There
29 is a slight improvement in the r^2 correlation coefficient between species modelled by the emission factor sensitivity
30 test for SPS1 and SPS2.

31

32 **4 Summary and Conclusions**

33 MEGANv2.1 has been incorporated into the CSIRO Chemical Transport Model. The CTM used a nested grid
34 approach, downscaling from an Australia wide domain to focus on receptor sites at a resolution of 3 km. This high
35 resolution simulation required a new plant functional type map to be constructed for Australia from an IGBP 1km
36 dataset. Whilst deconstructing the IGBP dataset to fit the NCAR PFTs has been done in accordance with literature
37 and local knowledge, it is subjective and may have introduced uncertainty. The model was used to predict
38 concentrations measured during four field campaigns in southeast Australia; one in spring (Tumbarumba), two in

1 summer (SPS1 and MUMBA) and one in Autumn (SPS2). The observed concentrations of isoprene and
2 monoterpenes were of a broadly similar magnitude, which may indicate that southeast Australia holds an unusual
3 position where neither chemical species dominates. The model over-predicted isoprene concentrations (up to a
4 factor of 6) and under-predicted monoterpenes (up to a factor of 4). A short series of measured emission fluxes at
5 Tumbarumba showed that the model over-predicted isoprene fluxes by a factor of 3 and under-predicted
6 monoterpene fluxes by a factor of 4 at midday.

7 Southeast Australia is dominated by forested regions, and cities here are surrounded by a high source of BVOC
8 emissions. These BVOCs have the capacity to dominate atmospheric chemical processes in urban airsheds during
9 the high temperatures experienced in Australian summers. Southeast Australia has been considered a global
10 hotspot for isoprene emissions due to the presence of high emitting Eucalypt species (Guenther et al., 2012)
11 although our results indicate that Eucalypts may not emit as much isoprene as previously thought. The
12 MEGANv2.1 isoprene and monoterpene emission factors assigned to Eucalypts, 24 and 1.6 mg m⁻² h⁻¹
13 respectively, are higher than the global average value of all broadleaf evergreen temperate trees (10 and 0.99 mg
14 m⁻² h⁻¹, table 2 of Guenther et al., 2012) because not all broadleaf evergreen temperate trees have high isoprene
15 and monoterpene emissions.

16 While there is a limited understanding of all of the processes controlling biogenic VOC emissions, such as the
17 impact of droughts, which can lead to an inhibition of BVOC emissions (Sharkey and Loreto, 1993; Pegoraro et
18 al., 2007), the overall emission can be adjusted by revising the emission factor. A sensitivity study reduced the
19 emission factors of isoprene by 3 and increased the monoterpene emission factors by 3.5. The effects on the
20 modelled concentrations was roughly linear. This experiment showed that there is no single increase/decrease
21 factor which suits all locations/seasons found in southeast Australia, indicating that adjustment is needed not only
22 in the emission factors but also in the representations of the processes controlling emissions variations.

23 The MEGANv2.1 emission factors for Eucalyptus were primarily based on enclosure measurements of young
24 trees. Street et al. (1997) conducted field enclosure measurements of *Eucalyptus globulus* trees in a plantation in
25 Portugal and found that both isoprene and monoterpene emissions from a 7 year old tree were about 5 times lower
26 than the emissions of a year old sapling. Nunes and Pio (2001) compared emissions from two year old *Eucalyptus*
27 *globulus* saplings in the laboratory and 7 year old trees in a plantation and found the adult tree isoprene emissions
28 were about a third lower than that of the young tree. The isoprene emission rates of adult *E. globulus*, *E. grandis*
29 and *E. camaldulensis* trees measured by Winter et al. (2009) are a factor of four lower than the emissions that He
30 et al. (2000) measured from 2 year old potted saplings of the same three Eucalypt species. This is in good agreement
31 with the results of Street et al. (1997) and Nunes and Pio (2001). The monoterpene emission rates measured by
32 Winter et al. (2009) for adult trees, however, were a factor of four higher than the 2 year old saplings measured by
33 He et al. (2000). This does not agree with the findings of Street et al. (1997), but does agree with the higher than
34 predicted atmospheric concentration measured at the field sites described in this paper. These results suggest that
35 the MEGANv2.1 isoprene emission factors for Eucalypts are biased by being based on measurements of young
36 trees and should be decreased by up to a factor of four or five considering that the isoprene emitting canopy consists
37 primarily of adult trees. This would result in better agreement with the observed ambient isoprene concentrations
38 described above. The results of monoterpene enclosure studies are more inconclusive and are also difficult to

1 interpret due to artefacts associated with elevated emissions from disturbance of the monoterpene storage
2 structures (Winters et al. 2009).

3 In order to more accurately characterize the atmospheric chemistry, air quality and climate in Australia, further
4 observations and quantitative analysis of Australian BVOC emission rates are needed. Australia is biologically
5 diverse and the canopy and understory are composed of many other species in addition to Eucalypts. Satellite
6 column measurements of BVOC oxidation products such as formaldehyde and glyoxal are available and can be
7 useful for investigating regional and seasonal distributions of biogenic emissions (Palmer et al., 2003; Kaiser et
8 al., 2015). Direct flux measurements, using towers and aircraft eddy flux approaches, are needed to provide a direct
9 constraint on Australian BVOC emissions (Karl et al., 2013).

10

11 **Acknowledgements**

12 The NSW Environment Trust has provided support for this study through the “Atmospheric Particles in Sydney:
13 model-observation verification study”. CPW wishes to acknowledge the Australian Research Council for funding
14 as part of the Discovery Project DP110101948. KME wishes to thank R. Law for helpful discussions on plant
15 functional types in Australia; to P. Hoffman for assistance with CDO; all those from CSIRO and the University of
16 Wollongong for fieldwork participation; and to J. Fisher and L. Emmons for helpful comments on the manuscript.

17 The LAI data product was retrieved from MCD15A2 version 4 from the online Data Pool, courtesy of the NASA
18 Land Processes Distributed Active Archive Center (LP DAAC), USGS/Earth Resources Observation and Science
19 (EROS) Center, Sioux Falls, South Dakota, https://lpdaac.usgs.gov/data_access/data_pool.

20

1 References

- 2 Arneth, A., Schurgers, G., Lathiere, J., Duhl, T., Beerling, D. J., Hewitt, C. N., Martin, M., and Guenther, A.:
3 Global terrestrial isoprene emission models: sensitivity to variability in climate and vegetation, *Atmos Chem Phys*,
4 11, 8037-8052, DOI 10.5194/acp-11-8037-2011, 2011.
- 5 Ashworth, K., Wild, O., and Hewitt, C. N.: Sensitivity of isoprene emissions estimated using MEGAN to the time
6 resolution of input climate data, *Atmos Chem Phys*, 10, 1193-1201, 2010.
- 7 Ayers, G. P., and Gillett, R. W.: Isoprene Emissions from Vegetation and Hydrocarbon Emissions from Bushfires
8 in Tropical Australia, *J Atmos Chem*, 7, 177-190, Doi 10.1007/Bf00048045, 1988.
- 9 Belward, A. S., Estes, J. E., and Kline, K. D.: The IGBP-DIS global 1-km land-cover data set DISCover: A project
10 overview, *Photogramm Eng Rem S*, 65, 1013-1020, 1999.
- 11 Bonan, G. B., Levis, S., Kergoat, L., and Oleson, K. W.: Landscapes as patches of plant functional types: An
12 integrating concept for climate and ecosystem models, *Global Biogeochem Cy*, 16, Artn 1021, Doi
13 10.1029/2000gb001360, 2002.
- 14 Cope, M., Keywood, M., Emmerson, K., Galbally, I., Boast, K., Chambers, S., Cheng, M., Crumeyrolle, S., Dunne,
15 E., Fedele, F., Gillett, R. W., Griffiths, A., Harnwell, J., Katzfey, J., Hess, D., Lawson, S., Miljevic, B., Molloy,
16 S., Powell, J., Reisen, F., Ristovski, Z., Selleck, P., Ward, J., Zhang, C., and Seng, J.: The Sydney Particle Study.
17 CSIRO, Australia. Available at <http://www.environment.nsw.gov.au/aqms/sydparticlestudy.htm>, 2014.
- 18 Cope, M. E., Hess, G. D., Lee, S., Tory, K., Azzi, M., Carras, J., Lilley, W., Manins, P. C., Nelson, P., Ng, L.,
19 Puri, K., Wong, N., Walsh, S., and Young, M.: The Australian Air Quality Forecasting System. Part I: Project
20 description and early outcomes, *J Appl Meteorol*, 43, 649-662, Doi 10.1175/2093.1, 2004.
- 21 Corney, S., Grose, M., Bennett, J. C., White, C., Katzfey, J., McGregor, J., Holz, G., and Bindoff, N. L.:
22 Performance of downscaled regional climate simulations using a variable-resolution regional climate model:
23 Tasmania as a test case, *J Geophys Res-Atmos*, 118, 11936-11950, 10.1002/2013jd020087, 2013.
- 24 DECCW: Air emissions inventory for the Greater Metropolitan Region in New South Wales; Calendar year 2003,
25 2007.
- 26 Emmerson, K. M., and Evans, M. J.: Comparison of tropospheric gas-phase chemistry schemes for use within
27 global models, *Atmos Chem Phys*, 9, 1831-1845, DOI 10.5194/acp-9-1831-2009, 2009.
- 28 Emmons, L. K., Walters, S., Hess, P. G., Lamarque, J. F., Pfister, G. G., Fillmore, D., Granier, C., Guenther, A.,
29 Kinnison, D., Laepple, T., Orlando, J., Tie, X., Tyndall, G., Wiedinmyer, C., Baughcum, S. L., and Kloster, S.:
30 Description and evaluation of the Model for Ozone and Related chemical Tracers, version 4 (MOZART-4), *Geosci*
31 *Model Dev*, 3, 43-67, 2010.
- 32 Evans, R. C., Tingey, D. T., Gumpertz, M. L., and Burns, W. F.: Estimates of isoprene and monoterpene emissions
33 rates in plants, *Botanical Gazette*, 143, 304-310, 1982.
- 34 Fountoukis, C., and Nenes, A.: ISORROPIA II: a computationally efficient thermodynamic equilibrium model for
35 $K^+-Ca^{2+}-Mg^{2+}-NH_4^+-Na^+-SO_4^{2-}-NO_3^- -Cl^- -H_2O$ aerosols, *Atmos Chem Phys*, 7, 4639-4659, 2007.
- 36 Greenberg, J. P., Guenther, A. B., Petron, G., Wiedinmyer, C., Vega, O., Gatti, L. V., Tota, J., and Fisch, G.:
37 Biogenic VOC emissions from forested Amazonian landscapes, *Global Change Biol*, 10, 651-662, 10.1111/j.1365-
38 2486.2004.00758.x, 2004.
- 39 Griffin, R. J., Cocker, D. R., Seinfeld, J. H., and Dabdub, D.: Estimate of global atmospheric organic aerosol from
40 oxidation of biogenic hydrocarbons, *Geophys Res Lett*, 26, 2721-2724, Doi 10.1029/1999gl1900476, 1999.
- 41 Guenther, A., Hewitt, C. N., Erickson, D., Fall, R., Geron, C., Graedel, T., Harley, P., Klinger, L., Lerdau, M.,
42 Mckay, W. A., Pierce, T., Scholes, B., Steinbrecher, R., Tallamraju, R., Taylor, J., and Zimmerman, P.: A Global-
43 Model of Natural Volatile Organic-Compound Emissions, *J Geophys Res-Atmos*, 100, 8873-8892, Doi
44 10.1029/94jd02950, 1995.
- 45 Guenther, A., Otter, L., Zimmerman, P., Greenberg, J., Scholes, R., and Scholes, M.: Biogenic hydrocarbon
46 emissions from southern African savannas, *J Geophys Res-Atmos*, 101, 25859-25865, Doi 10.1029/96jd02597,
47 1996.

1 Guenther, A., Archer, S., Greenberg, J., Harley, P., Helmig, D., Klinger, L., Vierling, L., Wildermuth, M.,
2 Zimmerman, P., and Zitzer, S.: Biogenic hydrocarbon emissions and landcover/climate change in a subtropical
3 savanna, *Phys Chem Earth Pt B*, 24, 659-667, Doi 10.1016/S1464-1909(99)00062-3, 1999.

4 Guenther, A., Karl, T., Harley, P., Wiedinmyer, C., Palmer, P. I., and Geron, C.: Estimates of global terrestrial
5 isoprene emissions using MEGAN (Model of Emissions of Gases and Aerosols from Nature), *Atmos Chem Phys*,
6 6, 3181-3210, 2006.

7 Guenther, A. B., Monson, R. K., and Fall, R.: Isoprene and Monoterpene Emission Rate Variability - Observations
8 with Eucalyptus and Emission Rate Algorithm Development, *J Geophys Res-Atmos*, 96, 10799-10808, Doi
9 10.1029/91jd00960, 1991.

10 Guenther, A. B., Jiang, X., Heald, C. L., Sakulyanontvittaya, T., Duhl, T., Emmons, L. K., and Wang, X.: The
11 Model of Emissions of Gases and Aerosols from Nature version 2.1 (MEGAN2.1): an extended and updated
12 framework for modeling biogenic emissions, *Geosci Model Dev*, 5, 1471-1492, DOI 10.5194/gmd-5-1471-2012,
13 2012.

14 Harley, P., Otter, L., Guenther, A., and Greenberg, J.: Micrometeorological and leaf-level measurements of
15 isoprene emissions from a southern African savanna, *J Geophys Res-Atmos*, 108, Artn 8468
16 doi:10.1029/2002jd002592, 2003.

17 Harley, P., Eller, A., Guenther, A., and Monson, R. K.: Observations and models of emissions of volatile terpenoid
18 compounds from needles of ponderosa pine trees growing in situ: control by light, temperature and stomatal
19 conductance, *Oecologia*, 176, 35-55, 10.1007/s00442-014-3008-5, 2014.

20 He, C. R., Murray, F., and Lyons, T.: Monoterpene and isoprene emissions from 15 Eucalyptus species in
21 Australia, *Atmos Environ*, 34, 645-655, Doi 10.1016/S1352-2310(99)00219-8, 2000.

22 Heald, C. L., Henze, D. K., Horowitz, L. W., Feddema, J., Lamarque, J. F., Guenther, A., Hess, P. G., Vitt, F.,
23 Seinfeld, J. H., Goldstein, A. H., and Fung, I.: Predicted change in global secondary organic aerosol concentrations
24 in response to future climate, emissions, and land use change, *Journal of Geophysical Research*, 113,
25 10.1029/2007jd009092, 2008.

26 Heald, C. L., Wilkinson, M. J., Monson, R. K., Alo, C. A., Wang, G. L., and Guenther, A.: Response of isoprene
27 emission to ambient CO₂ changes and implications for global budgets, *Global Change Biol*, 15, 1127-1140, DOI
28 10.1111/j.1365-2486.2008.01802.x, 2009.

29 Hoffmann, T., Odum, J. R., Bowman, F., Collins, D., Klockow, D., Flagan, R. C., and Seinfeld, J. H.: Formation
30 of organic aerosols from the oxidation of biogenic hydrocarbons, *J Atmos Chem*, 26, 189-222, Doi
31 10.1023/A:1005734301837, 1997.

32 Houweling, S., Dentener, F., and Lelieveld, J.: The impact of nonmethane hydrocarbon compounds on
33 tropospheric photochemistry, *J Geophys Res-Atmos*, 103, 10673-10696, Doi 10.1029/97jd03582, 1998.

34 Kaiser, J., Wolfe, G. M., Min, K. E., Brown, S. S., Miller, C. C., Jacob, D. J., deGouw, J. A., Graus, M., Hanisco,
35 T. F., Holloway, J., Peischl, J., Pollack, I. B., Ryerson, T. B., Warneke, C., Washenfelder, R. A., and Keutsch, F.
36 N.: Reassessing the ratio of glyoxal to formaldehyde as an indicator of hydrocarbon precursor speciation, *Atmos
37 Chem Phys*, 15, 7571-7583, 10.5194/acp-15-7571-2015, 2015.

38 Kanawade, V. P., Jobson, B. T., Guenther, A. B., Erupe, M. E., Pressley, S. N., Tripathi, S. N., and Lee, S. H.:
39 Isoprene suppression of new particle formation in a mixed deciduous forest, *Atmos Chem Phys*, 11, 6013-6027,
40 10.5194/acp-11-6013-2011, 2011.

41 Karl, T., Misztal, P. K., Jonsson, H. H., Shertz, S., Goldstein, A. H., and Guenther, A. B.: Airborne Flux
42 Measurements of BVOCs above Californian Oak Forests: Experimental Investigation of Surface and Entrainment
43 Fluxes, OH Densities, and Damkohler Numbers, *J Atmos Sci*, 70, 3277-3287, 10.1175/Jas-D-13-054.1, 2013.

44 Kim, H. K., Woo, J. H., Park, R. S., Song, C. H., Kim, J. H., Ban, S. J., and Park, J. H.: Impacts of different plant
45 functional types on ambient ozone predictions in the Seoul Metropolitan Areas (SMAs), Korea, *Atmos Chem
46 Phys*, 14, 7461-7484, DOI 10.5194/acp-14-7461-2014, 2014.

47 Kirstine, W., Galbally, I., Ye, Y. R., and Hooper, M.: Emissions of volatile organic compounds (primarily
48 oxygenated species) from pasture, *J Geophys Res-Atmos*, 103, 10605-10619, Doi 10.1029/97jd03753, 1998.

49 Kirstine, W. V., and Galbally, I. E.: A simple model for estimating emissions of volatile organic compounds from
50 grass and cut grass in urban airsheds and its application to two Australian cities, *J Air Waste Manage*, 54, 1299-
51 1311, 2004.

- 1 Knote, C., Tuccella, P., Curci, G., Emmons, L., Orlando, J. J., Madronich, S., Baro, R., Jimenez-Guerrero, P.,
2 Luecken, D., Hogrefe, C., Forkel, R., Werhahn, J., Hirtl, M., Perez, J. L., San Jose, R., Giordano, L., Brunner, D.,
3 Yahya, K., and Zhang, Y.: Influence of the choice of gas-phase mechanism on predictions of key gaseous
4 pollutants during the AQMEII phase-2 intercomparison, *Atmos Environ*, 115, 553-568,
5 10.1016/j.atmosenv.2014.11.066, 2015.
- 6 Kowalczyk, E. A., Stevens, L., Law, R. M., Dix, M., Wang, Y. P., Harman, I. N., Haynes, K., Sribnovsky, J., Pak,
7 B., and Ziehn, T.: The land surface model component of ACCESS: description and impact on the simulated surface
8 climatology, *Aust Meteorol Ocean*, 63, 65-82, 2013.
- 9 Lathiere, J., Hauglustaine, D. A., Friend, A. D., De Noblet-Ducoudre, N., Viovy, N., and Folberth, G. A.: Impact
10 of climate variability and land use changes on global biogenic volatile organic compound emissions, *Atmos Chem*
11 *Phys*, 6, 2129-2146, 2006.
- 12 Lee, A., Schade, G. W., Holzinger, R., and Goldstein, A. H.: A comparison of new measurements of total
13 monoterpene flux with improved measurements of speciated monoterpene flux, *Atmos Chem Phys*, 5, 505-513,
14 2005.
- 15 Loreto, F., and Delfine, S.: Emission of isoprene from salt-stressed *Eucalyptus globulus* leaves, *Plant Physiol*, 123,
16 1605-1610, DOI 10.1104/pp.123.4.1605, 2000.
- 17 Maleknia, S. D., Bell, T. L., and Adams, M. A.: Eucalypt smoke and wildfires: Temperature dependent emissions
18 of biogenic volatile organic compounds, *Int J Mass Spectrom*, 279, 126-133, DOI 10.1016/j.ijms.2008.10.027,
19 2009.
- 20 Maleknia, S. D.: Mass spectroscopy's role in studies of volatile organic pollutants, *Comprehensive environmental*
21 *mass spectroscopy*, edited by: Lebedev, A. T., ILM Publications, UK, 2012.
- 22 McGregor, J. L., and Dix, M. R.: An updated description of the Conformal-Cubic atmospheric model, *High*
23 *Resolution Numerical Modelling of the Atmosphere and Ocean*, 51-75, Doi 10.1007/978-0-387-49791-4_4, 2008.
- 24 Millet, D. B., Guenther, A., Siegel, D. A., Nelson, N. B., Singh, H. B., de Gouw, J. A., Warneke, C., Williams, J.,
25 Eerdekens, G., Sinha, V., Karl, T., Flocke, F., Apel, E., Riemer, D. D., Palmer, P. I., and Barkley, M.: Global
26 atmospheric budget of acetaldehyde: 3-D model analysis and constraints from in-situ and satellite observations,
27 *Atmos Chem Phys*, 10, 3405-3425, DOI 10.5194/acp-10-3405-2010, 2010.
- 28 Muller, J. F., Stavrou, T., Wallens, S., De Smedt, I., Van Roozendaal, M., Potosnak, M. J., Rinne, J., Munger,
29 B., Goldstein, A., and Guenther, A. B.: Global isoprene emissions estimated using MEGAN, ECMWF analyses
30 and a detailed canopy environment model, *Atmos Chem Phys*, 8, 1329-1341, 2008.
- 31 Nguyen, K. C., Katzfey, J. J., and McGregor, J. L.: Downscaling over Vietnam using the stretched-grid CCAM:
32 verification of the mean and interannual variability of rainfall, *Clim Dynam*, 43, 861-879, 10.1007/s00382-013-
33 1976-5, 2014.
- 34 Nunes, T. V., and Pio, C. A.: Emission of volatile organic compounds from Portuguese *Eucalyptus* forests,
35 *Chemosphere - Global Change Science*, 3, 239-248, 2001.
- 36 Palmer, P. I., Jacob, D. J., Fiore, A. M., Martin, R. V., Chance, K., and Kurosu, T. P.: Mapping isoprene emissions
37 over North America using formaldehyde column observations from space, *J Geophys Res-Atmos*, 108, Artn 4180,
38 Doi 10.1029/2002jd002153, 2003.
- 39 Papiez, M. R., Potosnak, M. J., Goliff, W. S., Guenther, A. B., Matsunaga, S. N., and Stockwell, W. R.: The
40 impacts of reactive terpene emissions from plants on air quality in Las Vegas, Nevada, *Atmos Environ*, 43, 4109-
41 4123, 10.1016/j.atmosenv.2009.05.048, 2009.
- 42 Paton-Walsh, C., Guerette, E.-A., Kubiston, D., Humphries, R., Wilson, S., Rea, G., Shi, X., Griffith, D., Buchholz,
43 R., Dominick, D., Velazco, V., Galbally, I., Keywood, M., Lawson, S., Selleck, P., Cheng, M., Molloy, S., Bhujel,
44 M., Emmerson, K., Griffiths, A., Chambers, S., and Davy, P.: Overview of the MUMBA campaign: Measurements
45 of Urban, Marine and Biogenic Air., *Atmos Environ*, submitted.
- 46 Pegoraro, E., Potosnak, M. J., Monson, R. K., Rey, A., Barron-Gafford, G., and Osmond, C. B.: The effect of
47 elevated CO₂, soil and atmospheric water deficit and seasonal phenology on leaf and ecosystem isoprene emission,
48 *Funct Plant Biol*, 34, 774-784, Doi 10.1071/Fp07021, 2007.
- 49 Pfister, G. G., Emmons, L. K., Hess, P. G., Lamarque, J. F., Orlando, J. J., Walters, S., Guenther, A., Palmer, P.
50 I., and Lawrence, P. J.: Contribution of isoprene to chemical budgets: A model tracer study with the NCAR CTM
51 MOZART-4, *J Geophys Res-Atmos*, 113, Artn D05308, Doi 10.1029/2007jd008948, 2008.

- 1 Pierce, T., Geron, C., Bender, L., Dennis, R., Tonnesen, G., and Guenther, A.: Influence of increased isoprene
2 emissions on regional ozone modeling, *J Geophys Res-Atmos*, 103, 25611-25629, Doi 10.1029/98jd01804, 1998.
- 3 Poulter, B., Ciais, P., Hodson, E., Lischke, H., Maignan, F., Plummer, S., and Zimmermann, N. E.: Plant functional
4 type mapping for earth system models, *Geosci Model Dev*, 4, 993-1010, DOI 10.5194/gmd-4-993-2011, 2011.
- 5 Pugh, T. A. M., Ashworth, K., Wild, O., and Hewitt, C. N.: Effects of the spatial resolution of climate data on
6 estimates of biogenic isoprene emissions, *Atmos Environ*, 70, 1-6, DOI 10.1016/j.atmosenv.2013.01.001, 2013.
- 7 Sarwar, G., Luecken, D., Yarwood, G., Whitten, G. Z., and Carter, W. P. L.: Impact of an updated carbon bond
8 mechanism on predictions from the CMAQ modeling system: Preliminary assessment, *J Appl Meteorol Clim*, 47,
9 3-14, Doi 10.1175/2007jamc1393.1, 2008.
- 10 Sarwar, G., Appel, K. W., Carlton, A. G., Mathur, R., Schere, K., Zhang, R., and Majeed, M. A.: Impact of a new
11 condensed toluene mechanism on air quality model predictions in the US, *Geosci Model Dev*, 4, 183-193, DOI
12 10.5194/gmd-4-183-2011, 2011.
- 13 Sharkey, T. D., and Loreto, F.: Water-Stress, Temperature, and Light Effects on the Capacity for Isoprene
14 Emission and Photosynthesis of Kudzu Leaves, *Oecologia*, 95, 328-333, Doi 10.1007/Bf00320984, 1993.
- 15 Shrivastava, M. K., Lane, T. E., Donahue, N. M., Pandis, S. N., and Robinson, A. L.: Effects of gas particle
16 partitioning and aging of primary emissions on urban and regional organic aerosol concentrations, *Journal of*
17 *Geophysical Research*, 113, 10.1029/2007jd009735, 2008.
- 18 Simpson, D.: Biogenic Emissions in Europe .2. Implications for Ozone Control Strategies, *J Geophys Res-Atmos*,
19 100, 22891-22906, Doi 10.1029/95jd01878, 1995.
- 20 Sindelarova, K., Granier, C., Bouarar, I., Guenther, A., Tilmes, S., Stavrou, T., Muller, J. F., Kuhn, U., Stefani,
21 P., and Knorr, W.: Global data set of biogenic VOC emissions calculated by the MEGAN model over the last 30
22 years, *Atmos Chem Phys*, 14, 9317-9341, DOI 10.5194/acp-14-9317-2014, 2014.
- 23 Situ, S., Guenther, A., Wang, X., Jiang, X., Turnipseed, A., Wu, Z., Bai, J., and Wang, X.: Impacts of seasonal
24 and regional variability in biogenic VOC emissions on surface ozone in the Pearl River delta region, China, *Atmos*
25 *Chem Phys*, 13, 11803-11817, DOI 10.5194/acp-13-11803-2013, 2013.
- 26 Spirig, C., Guenther, A., Greenberg, J. P., Calanca, P., and Tarvainen, V.: Tethered balloon measurements of
27 biogenic volatile organic compounds at a Boreal forest site, *Atmos Chem Phys*, 4, 215-229, 2004.
- 28 Stavrou, T., Muller, J. F., Bauwens, M., De Smedt, I., Van Roozendaal, M., Guenther, A., Wild, M., and Xia,
29 X.: Isoprene emissions over Asia 1979-2012: impact of climate and land-use changes, *Atmos Chem Phys*, 14,
30 4587-4605, DOI 10.5194/acp-14-4587-2014, 2014.
- 31 Stavrou, T., Muller, J. F., Bauwens, M., De Smedt, I., Van Roozendaal, M., De Maziere, M., Vigouroux, C.,
32 Hendrick, F., George, M., Clerbaux, C., Coheur, P. F., and Guenther, A.: How consistent are top-down
33 hydrocarbon emissions based on formaldehyde observations from GOME-2 and OMI?, *Atmos Chem Phys*, 15,
34 11861-11884, 10.5194/acp-15-11861-2015, 2015.
- 35 Street, R. A., Hewitt, C. N., and Mennicken, S.: Isoprene and monoterpene emissions from a Eucalyptus plantation
36 in Portugal, *J Geophys Res-Atmos*, 102, 15875-15887, Doi 10.1029/97jd00010, 1997.
- 37 Taraborrelli, D., Lawrence, M. G., Crowley, J. N., Dillon, T. J., Gromov, S., Gross, C. B. M., Vereecken, L., and
38 Lelieveld, J.: Hydroxyl radical buffered by isoprene oxidation over tropical forests (vol 5, pg 190, 2012), *Nat*
39 *Geosci*, 5, 300-300, Doi 10.1038/Ngeo1433, 2012.
- 40 van Donkelaar, A., Martin, R. V., Park, R. J., Heald, C. L., Fu, T. M., Liao, H., and Guenther, A.: Model evidence
41 for a significant source of secondary organic aerosol from isoprene, *Atmos Environ*, 41, 1267-1274, DOI
42 10.1016/j.atmosenv.2006.09.051, 2007.
- 43 Winer, A. M., Fitz, D. R., Miller, P. R., Atkinson, R. W., Brown, D. E., Carter, W. P. L., Dodd, M. C., Johnson,
44 C. W., Myers, M. A., Neisess, K. R., Poe, M. P., and Stephens, E. R.: Investigation of the role of natural
45 hydrocarbons in photochemical smog formation in California, final report contract AO-056-32, California Air
46 Resources Board, Sacramento, California, February 1983., 1983.
- 47 Winters, A. J., Adams, M. A., Bleby, T. M., Rennenberg, H., Steigner, D., Steinbrecher, R., and Kreuzwieser, J.:
48 Emissions of isoprene, monoterpene and short-chained carbonyl compounds from Eucalyptus spp. in southern
49 Australia, *Atmos Environ*, 43, 3035-3043, DOI 10.1016/j.atmosenv.2009.03.026, 2009.

1 Zhang, H. Q., Pak, B., Wang, Y. P., Zhou, X. Y., Zhang, Y. Q., and Zhang, L.: Evaluating Surface Water Cycle
2 Simulated by the Australian Community Land Surface Model (CABLE) across Different Spatial and Temporal
3 Domains, J Hydrometeorol, 14, 1119-1138, 10.1175/Jhm-D-12-0123.1, 2013.

4

5

6

7

8

9

10

11

12

13

14

15

16

17

18

19

20

21

22

23

24

25

26

27

28

29

30

31

1 Table 1 Model set-up and list of model runs completed

	SPS1	SPS2	MUMBA	Tumbarumba
240 hour average Temperature, K	295	290	295	289
24 hour average PAR, $\mu\text{mol m}^{-2} \text{s}^{-1}$	437	305	485	500
Coarse grid PFT	X			
Base MEGAN run	X	X	X	X
Exchange 50% crops \rightarrow grass				X
Emission factors isoprene /3 monoterpenes x3.5	X	X	X	X
\pm 20% NO _x emissions*	X	X	X	X

2 * Shown in supplementary material.

3

4

5 Table 2 Average (min-max) observed isoprene and monoterpene concentrations at all four field sites.

Observations	Isoprene ppb	Monoterpenes ppb
SPS1	0.76 (0.09* -7.10)	0.44 (0.20* -2.74)
SPS2	0.63 (0.01-4.63)	0.46 (0.006-1.95)
MUMBA	0.28 (0.002-4.57)	0.12 (0.004*-1.39)
Tumbarumba	0.15 (0.02*-1.01)	0.20 (0.02*-1.79)

6 * values equate to half the limit of detection.

7

8

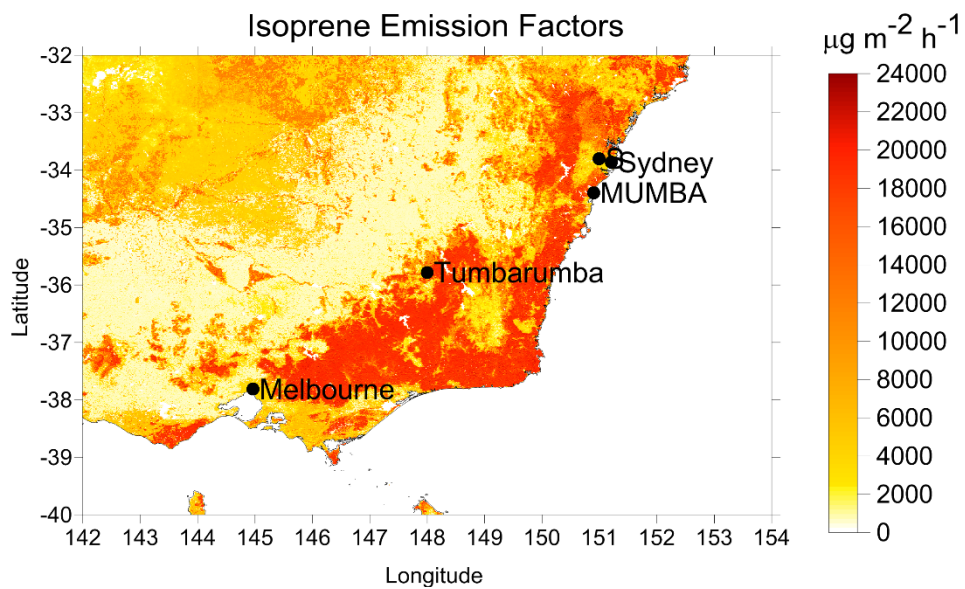
9

10

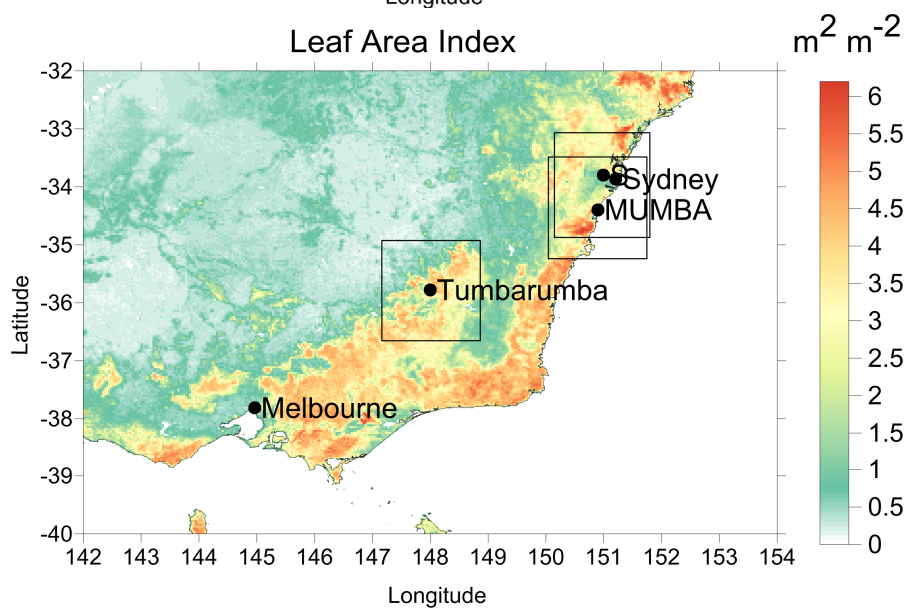
11

12

13

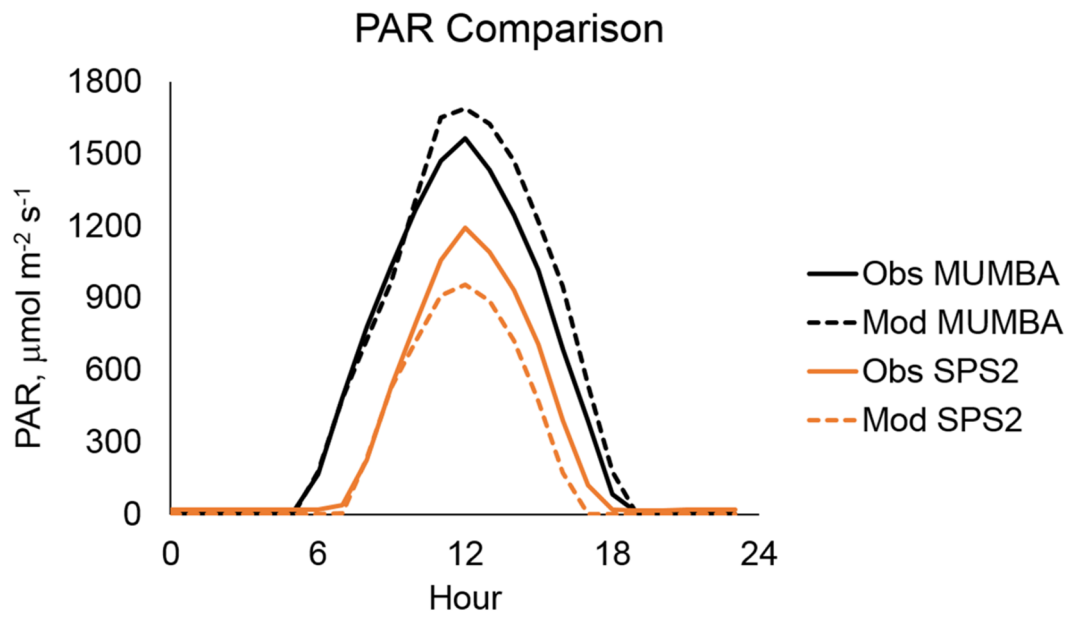


1



2

3 Figure 1 Southeast Australia at 1km resolution, showing (top) Isoprene from the MEGAN global emission factor
 4 map and (bottom) LAI in January, with the boundaries of the inner model domains marked. Major cities and the
 5 field campaign locations are also shown. The Sydney field campaigns were located west of Sydney marker.



1

2 Figure 2 Comparison of photosynthetically active radiation for modelled and measured SPS2 and MUMBA data.

3

4

5

6

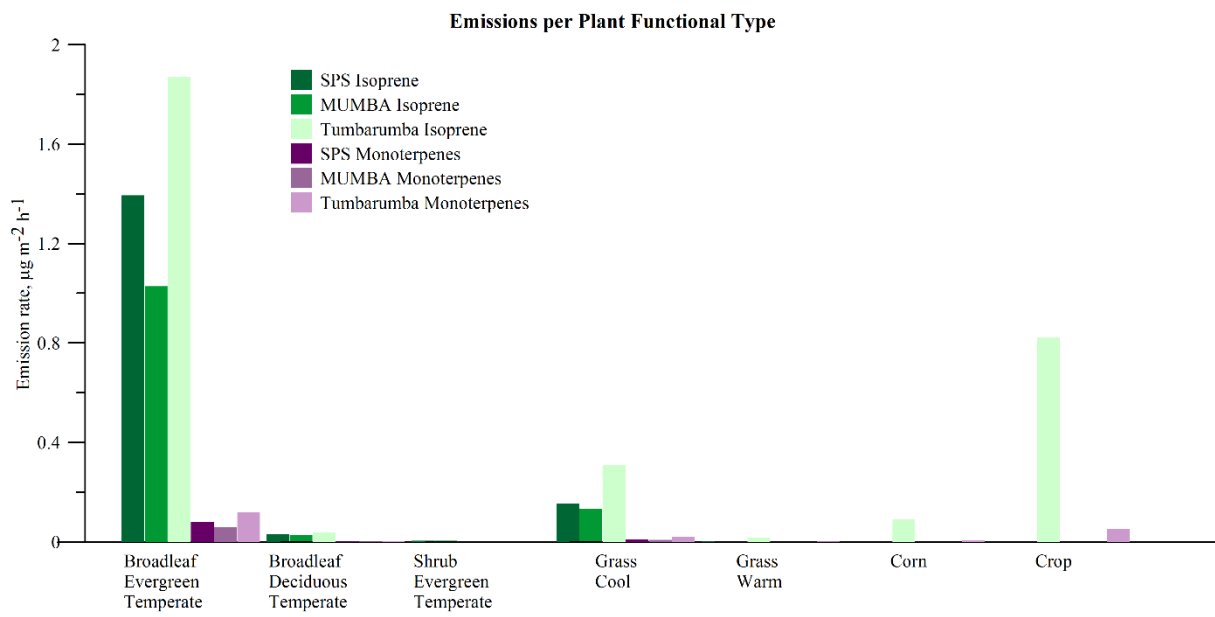
7

8

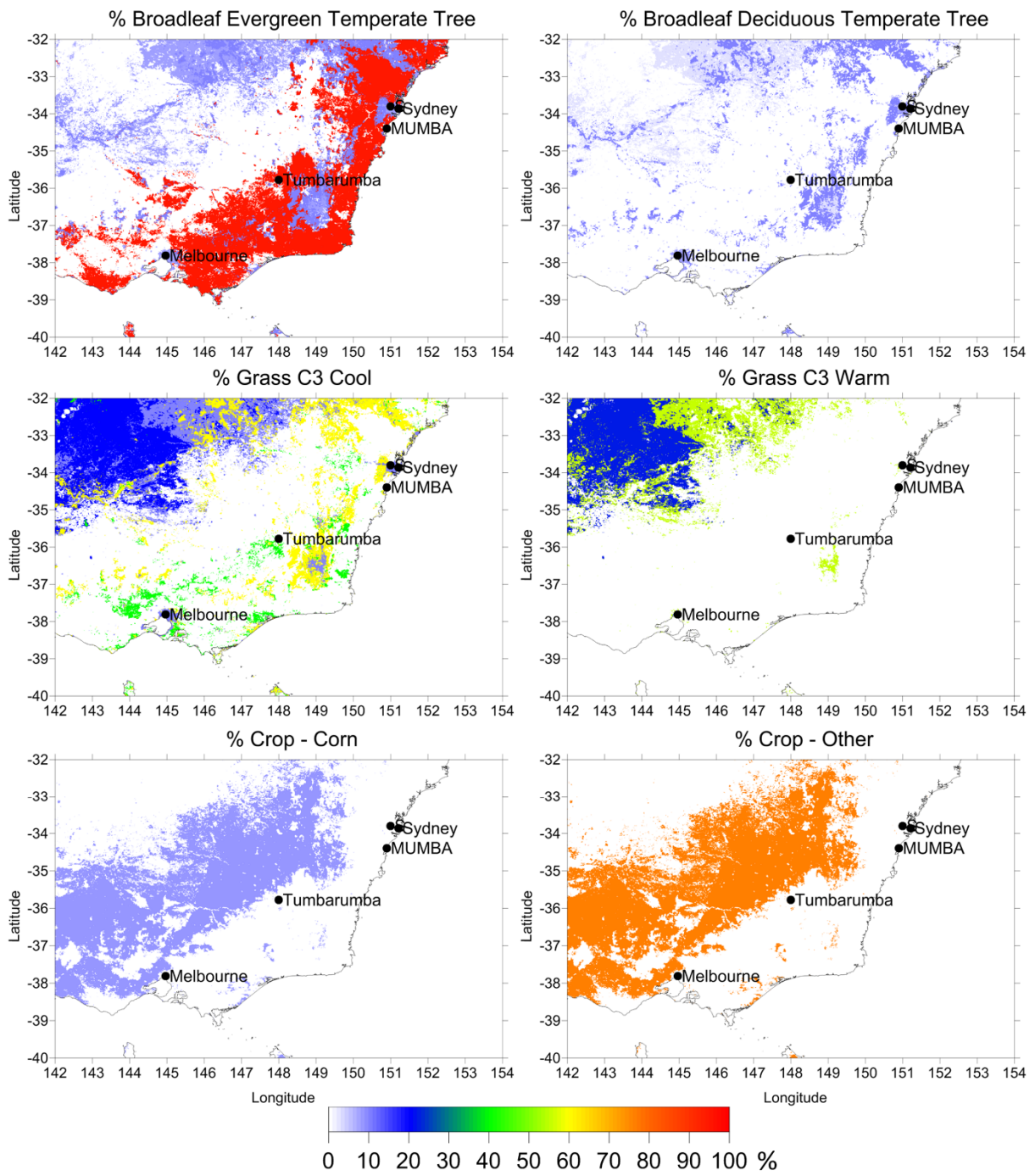
9

10

11

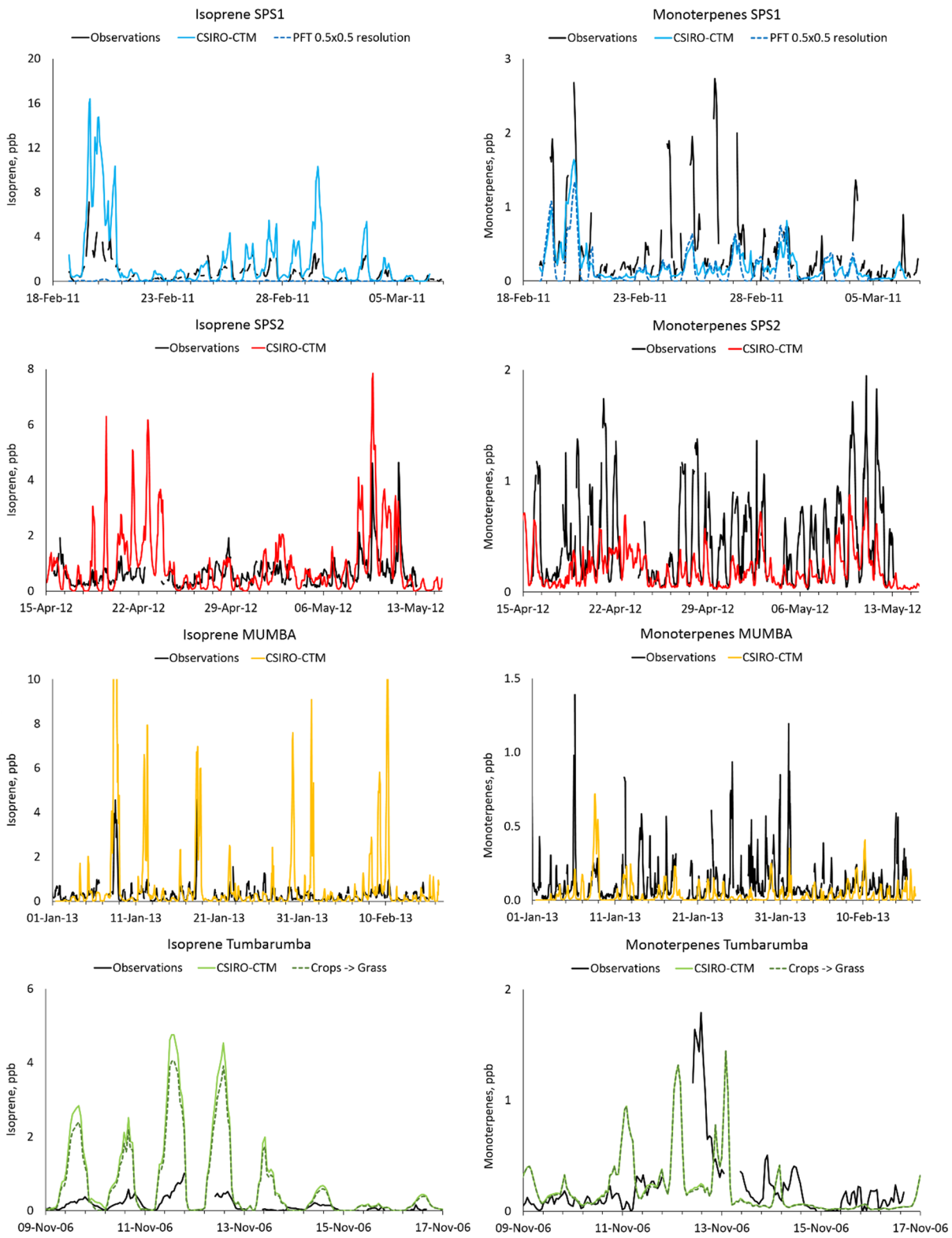


1
 2 Figure 3 The percentage area covered by the indicated PFTs resulting from splitting the 1km IGBP database into
 3 NCAR PFTs in southeast Australia.



1

2 Figure 4 Emission rates of isoprene and monoterpenes per PFT within each campaign's inner domain (180km x
 3 180 km).

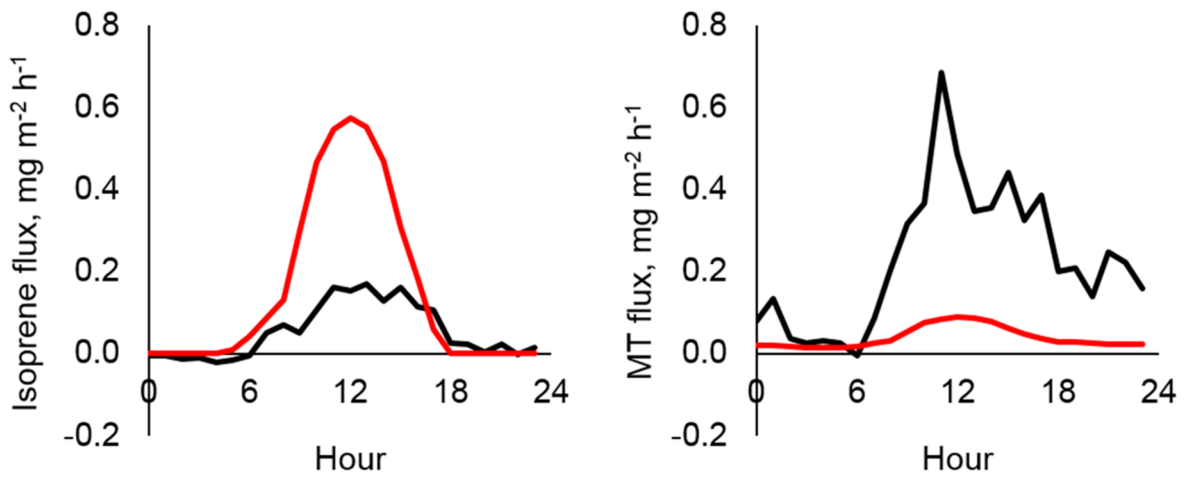


1

2 Figure 5 Time series of observed and modelled isoprene (left) and monoterpenes (right) for each field campaign.

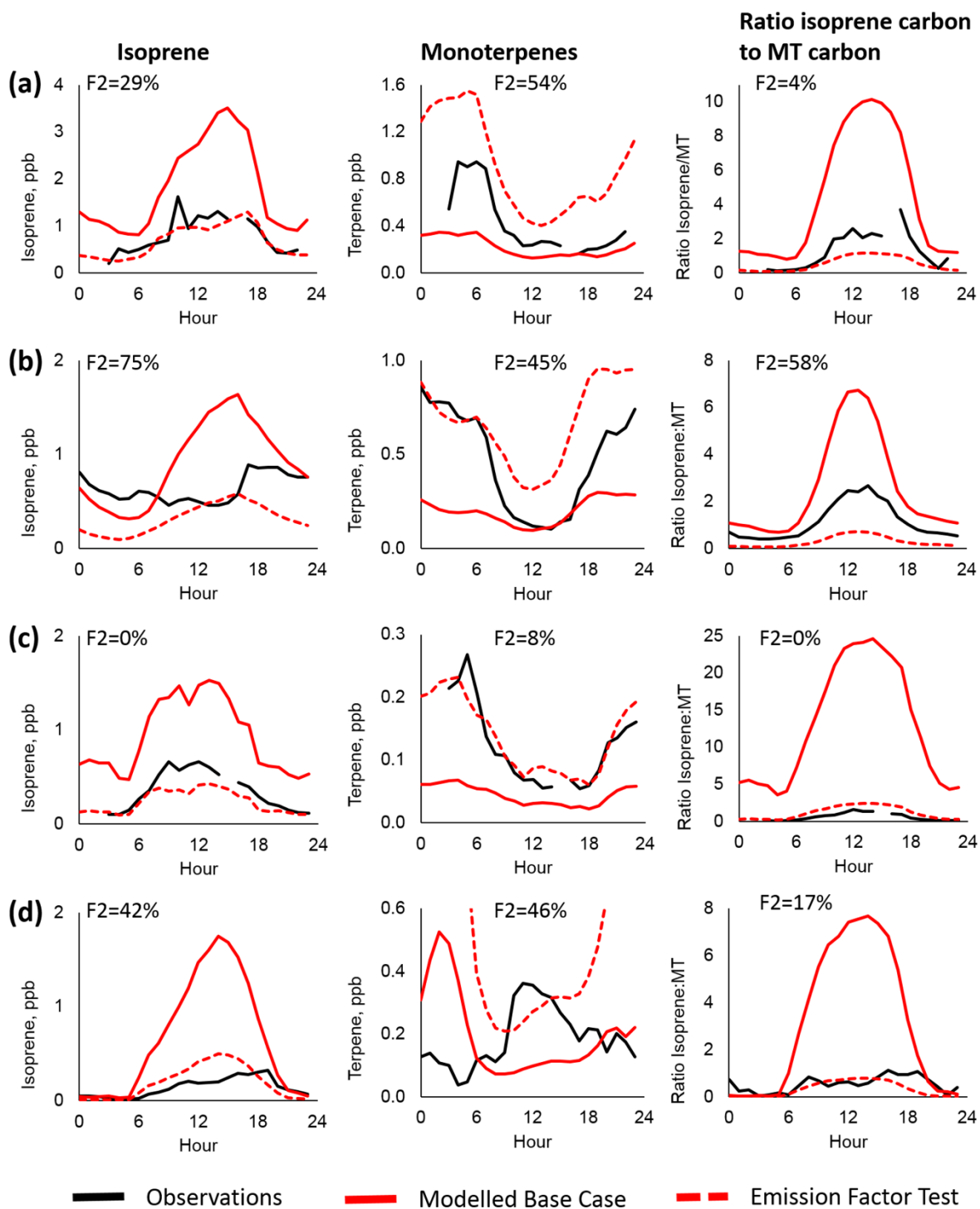
3 SPS1 = blue, SPS2 = red, MUMBA = yellow, Tumbarumba = green. Y-axis for isoprene during MUMBA

4 restricted to 10ppb, as modelled peak is 38 ppb on 8.1.13.



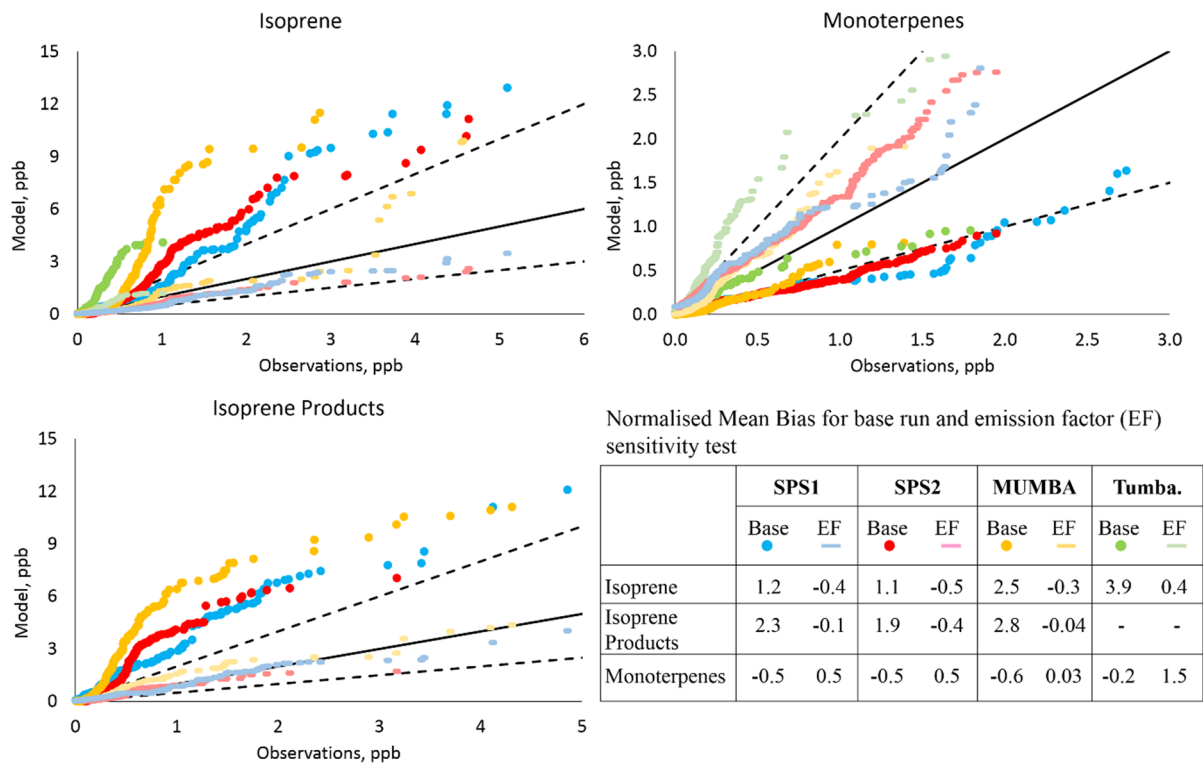
1

2 Figure 6 Diurnal cycles of isoprene (left) and monoterpene (MT, right) emission fluxes from three days of eddy
 3 covariance measurements at Tumbarumba during November 2006. Modelled emission fluxes are plotted from the
 4 same time period.



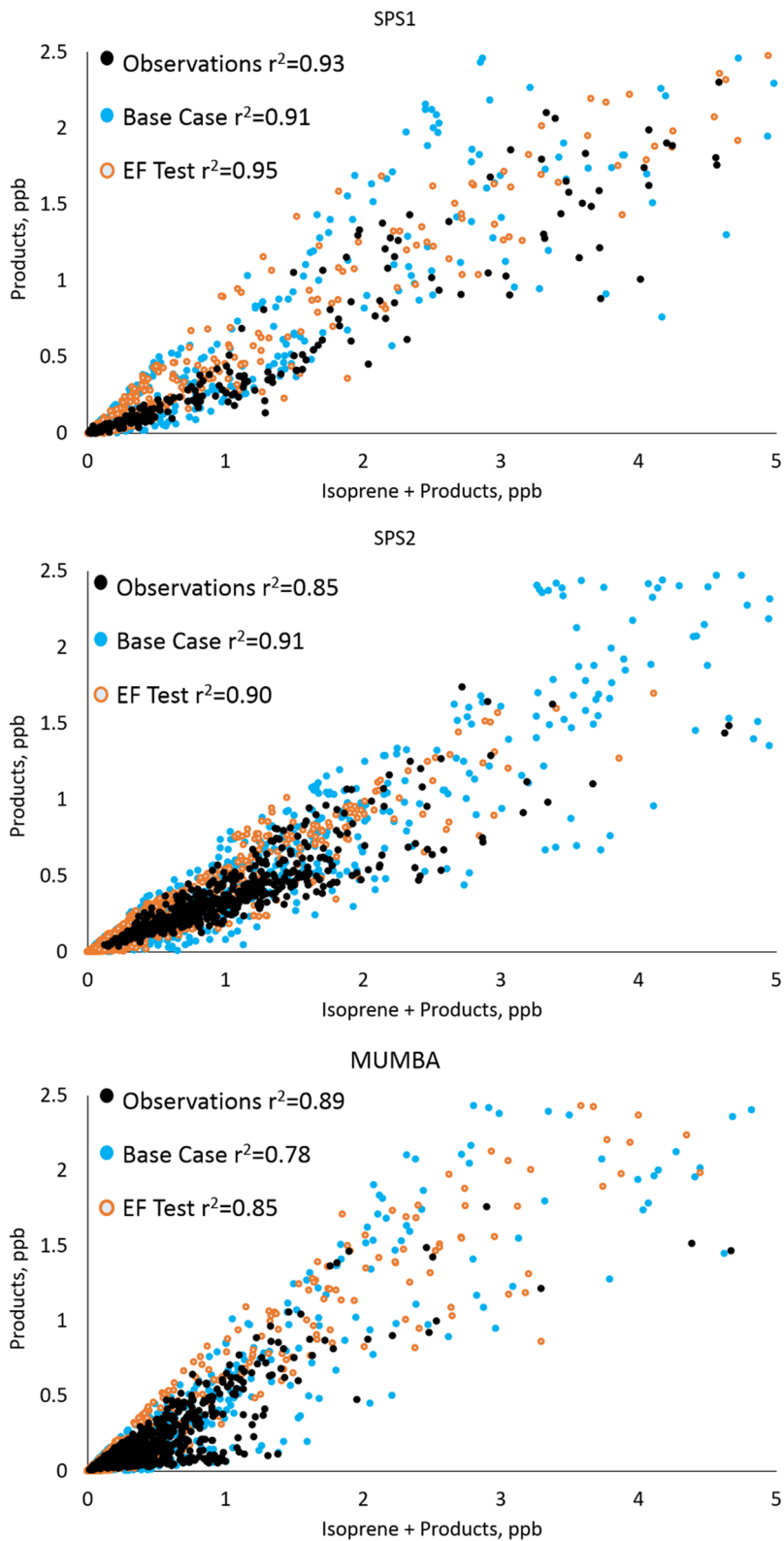
1

2 Figure 7 Campaign average diurnal cycles for isoprene (left), monoterpenes (middle) and the ratio of isoprene
 3 carbon to monoterpenes (MT) carbon (right). (a)=SPS1, (b)=SPS2, (c)=MUMBA (d)=Tumberumba. F2=
 4 percentage within a factor of 2 between observations and base run.



1

2 Figure 8 Quantile-quantile plots to show relationship between modelled and observed biogenic gases. The base
 3 run are dots, the emission factor sensitivity study are the dashes. The solid black line = 1:1; dashed black lines
 4 indicate \pm a factor of 2. Note: isoprene products are MVK + MACR. The y-axis on isoprene chart is reduced to 15
 5 ppb to aid visual comparison, as modelled MUMBA data reaches 38 ppb.



1

2 Figure 9 Scatterplots of modelled and observed ratios between isoprene and the isoprene products, with r^2
 3 correlation coefficients. EF = emission factor sensitivity test. Note, x and y axes restricted to 5 ppb and 2.5 ppb
 4 respectively.